VIP Hydrogen Evolution Very Important Paper

International Edition: DOI: 10.1002/anie.201706921
German Edition: DOI: 10.1002/ange.201706921

Potential-Cycling Synthesis of Single Platinum Atoms for Efficient Hydrogen Evolution in Neutral Media

Lihan Zhang[+], Lili Han[+], Haoxuan Liu, Xijun Liu, and Jun Luo**

Abstract: *Single-atom catalysts (SACs) have exhibited high activities for the hydrogen evolution reaction (HER) electrocatalysis in acidic or alkaline media, when they are used with binders on cathodes. However, to date, no SACs have been reported for the HER electrocatalysis in neutral media. We demonstrate a potential-cycling method to synthesize a catalyst comprising single Pt atoms on CoP-based nanotube arrays supported by a Ni foam, termed PtSA-NT-NF. This binder-free catalyst is centimeter-scale and scalable. It is directly used as HER cathodes, whose performances at low and high current densities in phosphate buffer solutions (pH 7.2) are comparable to and better than, respectively, those of commercial Pt/C. The Pt mass activity of PtSA-NT-NF is 4 times of that of Pt/C, and its electrocatalytic stability is also better than that of Pt/C. This work provides a large-scale production strategy for binder-free Pt SAC electrodes for efficient HER in neutral media.*

Single-atom catalysts (SACs) have recently attracted much attention,[1] owing to their maximum usage of metal atoms and great potential to achieve high activities for catalyzing the CO oxidation,[2,3] water-gas shift,[2a,4] oxidation of benzene,[5] oxygen reduction reaction,[6] carbon dioxide reduction,[7] triiodide reduction,[8] oxygen evolution reaction,[9] and hydrogen evolution reaction (HER).[10–13] Among these reactions, the electrocatalytic HER[11–13] is one of the green and sustainable approaches to generate molecular hydrogen (H_2), a clean energy carrier. Thus, a variety of synthetic approaches, such as chemical vapor deposition,[12a] atomic layer deposition,[12b] pyrolysis[12c,13a] and wet chemistry method,[13b,c] have been developed to fabricate SACs including single Ni atoms on graphene (NiSA-graphene),[12a] PtSA-graphene,[12b] NiSA-carbon,[12c] CoSA-graphene,[13a] Pt/Co/NiSA-MoS_2,[13b] and PtSA-TiWC.[13c] These catalysts exhibited breakthrough performances for the HER electrocatalysis in acidic or alkaline media, when they were applied with binders on cathodes.[11a,d,12,13] However, up to now, no SACs have been reported for the HER electrocatalysis in neutral media.

Commercial Pt/C catalysts consisting of Pt nanoparticles on carbon have been recognized to be the most effective benchmark for the HER electrocatalysis in neutral media.[14] If Pt SACs are realized for this field, higher activities should be achieved, because of their higher mass utilization and the positive modulation of their electronic structures by substrates.[11b,c,13b,c] It has been reported that Pt atoms can be dissolved from Pt anodes into acid or alkaline media at high voltages and then transferred onto cathodes.[15,16]

Motivated by the above breakthroughs, we develop a potential-cycling method with a three-electrode cell containing phosphate buffer solution (PBS) to synthesize a catalyst that comprises large-area Pt SACs on CoP-based nanotube (NT) arrays supported by a Ni foam (NF), termed PtSA-NT-NF. This catalyst has centimeter-scale dimensions, which are scalable. Each PtSA-NT-NF piece can be directly used as an electrocatalytic HER cathode, in which no binders are needed. In PBS, PtSA-NT-NF exhibits an ultralow overpotential (η) of 24 mV for the HER current density (j_{HER}) of 10 mA cm^{-2}, only 7 mV larger than that of commercial Pt/C. More importantly, PtSA-NT-NF shows multiple performances better than Pt/C: at $j_{HER} > 43$ mA cm^{-2}, its η values are prominently smaller and thus better than those of Pt/C; its Pt mass activity at $\eta = 50$ mV is 70 Ag^{-1}, four-times of that of Pt/C; its Tafel slope is only 30 mV dec^{-1}, as good as that of Pt/C (31 mV dec^{-1}); its high activity was maintained for 24 h in the chronoamperometric test, also more stable than that of Pt/C. These results may help accelerate the large-scale binder-free application of Pt SACs and efficient HER.

Figure 1 a displays the process to synthesize PtSA-NT-NF. Briefly, in a three-electrode cell containing 1 M PBS (pH 7.2), the CE, RE, and WE are a Pt foil, a saturated calomel electrode (SCE), and a NF with CoP-based nanorod/nanosheet arrays on its surface (which is a precursor sample, denoted as S1; see the Experimental Section and Figure S1 in the Supporting Information for details), respectively. In the cell, potential cycling was performed with the scan rate of 150 mV s^{-1} between −1.5 and −0.668 V vs. SCE at 25 °C (all other potential values in this work are vs. reversible hydrogen electrode, RHE). Figure 1 b gives the HER polarization curves of S1 after 0, 2500, 5000, 7500, and 10000 potential cycles were performed. The first three curves are remarkably different from each other, indicating that the HER electrocatalytic performance of S1 and thus its structure changed during the first 5000 cycles. After the 5000 cycles, the changing trend faded, suggesting that the structure of S1 became

[*] L. H. Zhang,[+] Dr. L. L. Han,[+] H. X. Liu, Dr. X. J. Liu, Prof. J. Luo
Center for Electron Microscopy, TUT-FEI Joint Laboratory, Tianjin Key Laboratory of Advanced Functional Porous Materials, Institute for New Energy Materials & Low-Carbon Technologies, School of Materials Science and Engineering, Tianjin University of Technology
Tianjin 300384 (China)
E-mail: xjliu@tjut.edu.cn
jluo@tjut.edu.cn

[+] These authors contributed equally to this work.

Supporting information for this article can be found under: https://doi.org/10.1002/anie.201706921.

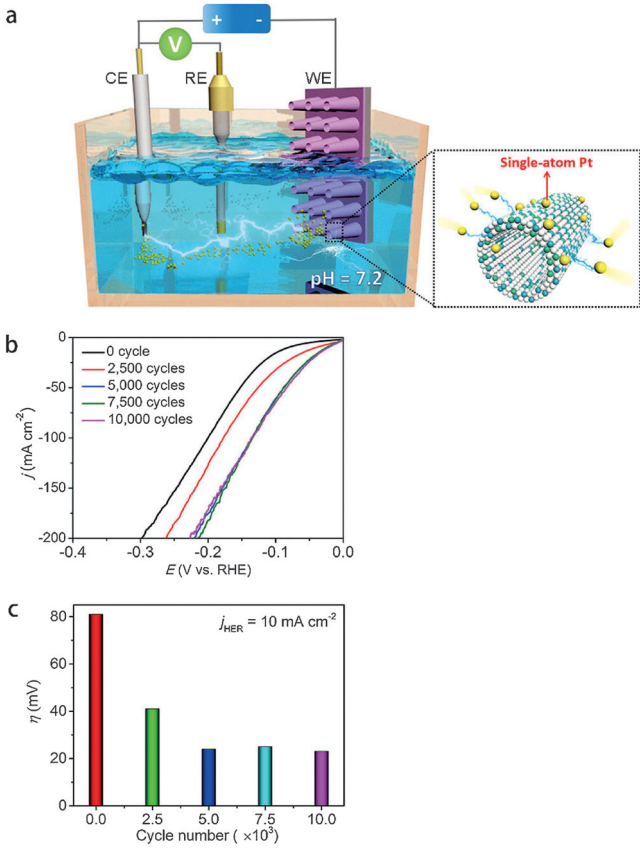

Figure 1. a) Schematic diagram of the synthesis process. CE counter electrode, RE reference electrode, WE working electrode. The CE is Pt. b) HER polarization curves of the S1 precursor sample after different numbers of potential cycles were performed on it. The curves were taken with 5 $mV s^{-1}$ in N_2-saturated 1 M PBS at 25 °C. c) Dependence of the overpotential of S1 on the cycle number.

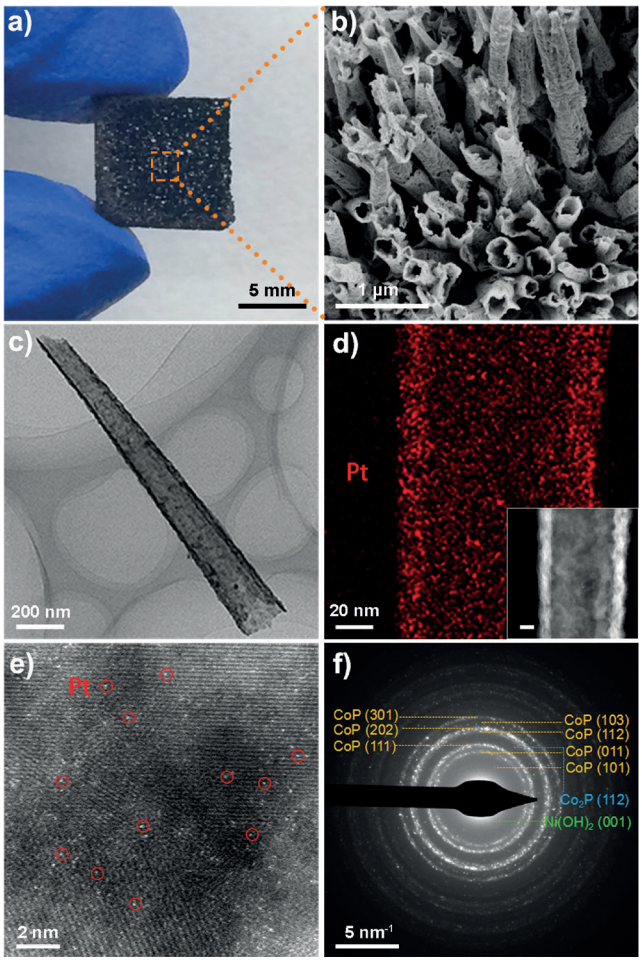

Figure 2. a),b) Optical and SEM images of a piece of PtSA-NT-NF. c) TEM image of a NT from the piece of PtSA-NT-NF. d) EDS map of Pt in a NT. The inset is the corresponding high-angle annular dark field (HAADF) image scale bar: 20 nm. e) Atomic-resolution (AR) HAADF image of the NT in (d) (Pt atoms ringed in red; more AR images are in Figure S3). f) Electron diffraction pattern of NTs.

stable. Figure 1c shows the dependence of η driving $j_{HER} = 10\ mA\,cm^{-2}$ on the cycle number. The η values at $j_{HER} = 10\ mA\,cm^{-2}$ have been widely used to evaluate the HER electrocatalytic performance, with smaller values indicating higher HER activities.[17] Thus, Figure 1c indicates that the potential cycling promoted the HER activity of S1 up to 5000 cycles. Therefore, we used the 5000 potential cycles to transform each precursor sample into a desired one, which was later found to be PtSA-NT-NF.

Figure 2a–c shows the optical, scanning electron microscopic (SEM), and transmission electron microscopic (TEM) images of a piece of sample after the 5000 potential cycles. This sample has centimeter-scale dimensions and contains an array of NTs standing on a NF. The centimeter-scale dimensions are determined by the sizes of the three-electrode cell and the autoclave for producing the precursors, and thus are scalable. The NTs have diameters of around 140 nm and wall thicknesses of around 20 nm. The energy dispersive X-ray spectroscopic (EDS) result in Figure 2d shows the presence of Pt in the NTs (see Figure S2 for the EDS maps of Co, Mn, O, P, and Ni), and the Pt weight percentage is 1.6%. AR HAADF imaging performed by aberration-corrected scanning TEM (STEM) indicates that a plenty of single Pt atoms are well dispersed on the NTs (Figures 2e and Figure S3), similar to those reported,[10a,c,12,13,18] and no Pt crystal grains/particles are found. Further, the electron diffraction pattern in Figure 2f demonstrates that the NTs contain the crystal grains of $Ni(OH)_2$, CoP and Co_2P, but no diffraction spots from Pt crystals are present, according to the standard crystallographic data of Joint Committee on Powder Diffraction Standards. This result is consistent with the X-ray diffraction (XRD) pattern of a centimeter-scale piece of PtSA-NT-NF (Figure 3a), which contains the signals of not Pt but $Ni(OH)_2$, CoP, and Co_2P crystal grains. Moreover, as shown in Figure 3b, the X-ray photoelectron spectrum (XPS) of commercial Pt/C containing Pt nanoparticles displays two Pt 4f peaks at 71.6 and 74.9 eV, indicative of Pt^0 (Refs [4b,13c,19]). In contrast, the two Pt 4f peaks of a centimeter-scale piece of PtSA-NT-NF are located at 72.3 and 75.6 eV, which are characteristic of Pt^{2+} (Refs. [4b,13c,19]). The lack of a detectable Pt^0 signal implies that not Pt crystal grains but only single Pt atoms exist in PtSA-NT-NF, conforming to the absence of Pt crystal grain signals in the XRD and the electron diffraction patterns. The

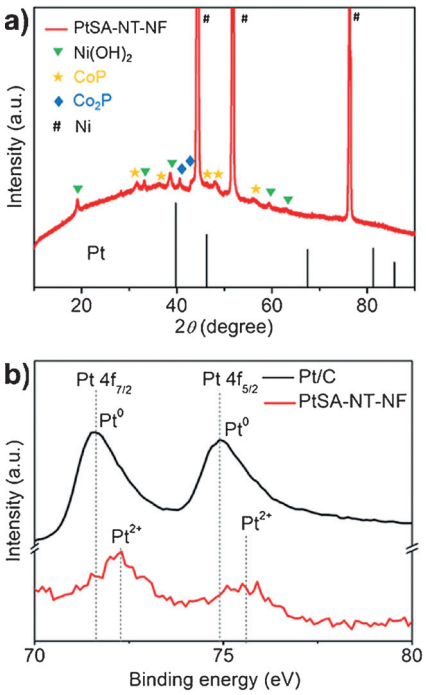

Figure 3. a) XRD pattern of PtSA-NT-NF (red) and the standard one of Pt (black). b) XPS spectra of PtSA-NT-NF and commercial 20 wt% Pt/C.

2+ valence of Pt^{2+} originates from the interaction between single Pt atoms and substrates.[13c]

Because single Pt atoms in each piece of PtSA-NT-NF are distributed on NTs supported by a large NF, each PtSA-NT-NF piece with the single atoms can be directly used as an HER cathode, and no binders are needed. Figure 4a gives the HER polarization curves of commercial Pt/C, a PtSA-NT-NF sample, a pure NF and a NF with CoP-based NT arrays and without single Pt atoms (termed NT-NF), whose synthesis is similar to that of PtSA-NT-NF (see details in the Experimental Section in the Supporting Information). The NTs in NT-NF are nearly identical to those in PtSA-NT-NF (Figure S4). According to Figure 4a, the η values at $j_{HER} = 10\ mA\,cm^{-2}$ are 337 mV for NF, 46 mV for NT-NF, 24 mV for PtSA-NT-NF, and 17 mV for Pt/C, indicating that the single Pt atoms contribute much to the HER performance of PtSA-NT-NF. It is worth noting that the η value of PtSA-NT-NF is only 7 mV larger than that of Pt/C and much smaller than those of reported HER catalysts (Table S1), indicating an efficient HER performance in neutral media. More importantly, Figure 4a shows that PtSA-NT-NF exhibits much smaller η values than commercial Pt/C at $j_{HER} > 43\ mA\,cm^{-2}$, suggesting that the HER performance of PtSA-NT-NF at high current densities is better than that of Pt/C.

Figure 4b shows that the Tafel slopes of NF, NT-NF, PtSA-NT-NF, and Pt/C are 160, 38, 30, and 31 $mV\,dec^{-1}$, respectively. These results indicate that the HER performance on NF was poor, the HER on NT-NF occurred through the Volmer-Heyrovsky mechanism with the electrochemical combination of an adsorbed hydrogen atom, a free proton and a free electron as the rate-limiting step (RLS),[20] and the HER on both PtSA-NT-NF and Pt/C did through the Volmer–Tafel mechanism with the recombination between the adjacent adsorbed hydrogen atoms as the RLS.[21]

The electrochemically active surface area (ECSA) values of NT-NF, PtSA-NT-NF, and Pt/C were measured to be 39.6, 76.1, and 29.4 cm^2, respectively (see details in the Experimental Section in the Supporting Information and Figure S5). The largest ECSA value of PtSA-NT-NF implies the presence of more active sites than NT-NF and Pt/C. In addition, the specific surface area (SSA) value of PtSA-NT-NF is close to that of NT-NF, and micropores and mesopores exist in both of them (Figure S6). These findings confirm that the NT arrays in PtSA-NT-NF and NT-NF have nearly identical structures, as shown in Figures 2b,c, Figure S2 and Figure S4, except the presence of single Pt atoms only in PtSA-NT-NF. Thus, the larger ECSA value of PtSA-NT-NF should be caused by the presence of single Pt atoms. Furthermore, the Pt loading of PtSA-NT-NF was determined by inductively coupled plasma optical emission spectroscopy (ICP-OES) to be 1.76 wt%. Then, by normalizing activities to the Pt loadings and deducting the contributions of the NTs and NFs (see the Experimental Section for details), the HER mass activities of Pt/C and single Pt atoms on PtSA-NT-NF were given to be 17 and 70 $A\,g^{-1}$, respectively, at $\eta = 50$ mV (this overpotential was chosen by following Ref. [12b]). The value for single Pt atoms on PtSA-NT-NF is four times that of Pt/C, indicating the more efficient HER performance of the single Pt atoms. Figure 4d shows that PtSA-NT-NF maintained a stable HER performance over 24 h, whereas the

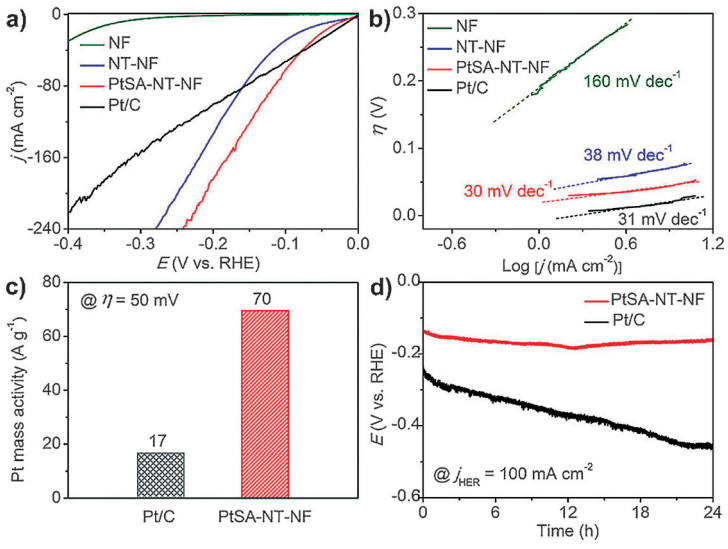

Figure 4. a) HER polarization curves of NF, NT-NF, PtSA-NT-NF, and Pt/C, acquired with 5 $mV\,s^{-1}$ in N_2-saturated 1 M PBS at 25 °C. b) Tafel plots of the polarization curves in (a). c) Pt mass activities of PtSA-NT-NF and Pt/C at $\eta = 50$ mV. The activity values have been normalized to the Pt loadings, and the contributions of the NTs and NFs have been deducted. d) Chronoamperometric curves of PtSA-NT-NF and Pt/C at a constant $j_{HER} = 100\ mA\,cm^{-2}$. The CEs used for the results in (a–d) are all graphite rods.

performance of Pt/C degraded remarkably. Moreover, the η value of PtSA-NT-NF at $j_{HER} = 10\ mA\,cm^{-2}$ after the stability test shows a small increase of 8 mV, much smaller than the increase of Pt/C, 128 mV (Figure S7). These results demonstrate the high stability of PtSA-NT-NF, which is also verified by its stable structure and electrocatalytic kinetics (Figures S8 and S9). The above findings suggest that the single Pt atoms possess better HER performances than Pt/C in neutral media, which should originate from the high Pt mass utilization and the positive modulation of the SAC electronic structures by substrates.[11b,c,13b,c] Moreover, no influences from binders exist in our measurements. Besides, we examined the HER performances of PtSA-NT-NF in acidic and alkaline media, and the results indicate that it is also a good electrocatalyst for the HER in acidic and alkaline media (Figure S10). The potential-cycling synthesis was also performed on nanoporous gold (NPG),[15c] by which Pt atoms were deposited onto NPG (Figure S11).

In summary, we have successfully synthesized a PtSA-NT-NF catalyst, which comprises single Pt atoms without Pt grains/particles on CoP-based NTs supported by a NF, using potential cycling in neutral media. The dimensions of each PtSA-NT-NF piece are centimeter-scale and can be further scaled up. PtSA-NT-NF can be directly used as electrocatalytic HER cathodes in neutral media, and no binders are needed. The catalyst is the first type of SACs used for the HER electrocatalysis in neutral media, and it exhibits $\eta =$ 24 mV for $j_{HER} = 10\ mA\,cm^{-2}$, comparable to commercial Pt/C (17 mV), which is the best HER electrocatalyst. More strikingly, the η values of PtSA-NT-NF are much smaller and thus better than those of Pt/C at $j_{HER} > 43\ mA\,cm^{-2}$, its Pt mass activity at $\eta = 50$ mV is four times that of Pt/C, its Tafel slope is only $30\ mV\,dec^{-1}$, as good as that of Pt/C, and it has a better durability than Pt/C. These results provide a promising approach for synthesizing large-area, binder-free and scalable Pt SAC electrodes for high-performance catalysis.

Acknowledgements

This work was financially supported by National Natural Science Foundation of China (21601136 & 51572016), National Program for Thousand Young Talents of China, Tianjin Municipal Education Commission, and Tianjin Municipal Science and Technology Commission (15JCYBJC52600).

Conflict of interest

The authors declare no conflict of interest.

Keywords: electrode materials · hydrogen evolution reaction · platinum · potential cycling · single-atom catalysis

How to cite: *Angew. Chem. Int. Ed.* **2017**, *56*, 13694–13698
Angew. Chem. **2017**, *129*, 13882–13886

[1] J. Jones, H. Xiong, A. T. DeLaRiva, E. J. Peterson, H. Pham, S. R. Challa, G. Qi, S. Oh, M. H. Wiebenga, X. I. Pereira Hernández, Y. Wang, A. K. Datye, *Science* **2016**, *353*, 150–154.

[2] a) K. Ding, A. Gulec, A. M. Johnson, N. M. Schweitzer, G. D. Stucky, L. D. Marks, P. C. Stair, *Science* **2015**, *350*, 189–192; b) B. Qiao, A. Wang, X. Yang, L. F. Allard, Z. Jiang, Y. Cui, J. Liu, J. Li, T. Zhang, *Nat. Chem.* **2011**, *3*, 634–641.

[3] a) E. J. Peterson, A. T. DeLaRiva, S. Lin, R. S. Johnson, H. Guo, J. T. Miller, J. Hun Kwak, C. H. F. Peden, B. Kiefer, L. F. Allard, F. H. Ribeiro, A. K. Datye, *Nat. Commun.* **2014**, *5*, 4885; b) B. Qiao, J. Liu, Y.-G. Wang, Q. Lin, X. Liu, A. Wang, J. Li, T. Zhang, J. Liu, *ACS Catal.* **2015**, *5*, 6249–6254.

[4] a) J. Lin, A. Wang, B. Qiao, X. Liu, X. Yang, X. Wang, J. Liang, J. Li, J. Liu, T. Zhang, *J. Am. Chem. Soc.* **2013**, *135*, 15314–15317; b) M. Yang, J. Liu, S. Lee, B. Zugic, J. Huang, L. F. Allard, M. Flytzani-Stephanopoulos, *J. Am. Chem. Soc.* **2015**, *137*, 3470–3473.

[5] D. Deng, X. Chen, L. Yu, X. Wu, Q. Liu, Y. Liu, H. Yang, H. Tian, Y. Hu, P. Du, R. Si, J. Wang, X. Cui, H. Li, J. Xiao, T. Xu, J. Deng, F. Yang, P. N. Duchesne, P. Zhang, J. Zhou, L. Sun, J. Li, X. Pan, X. Bao, *Sci. Adv.* **2015**, *1*, e1500462.

[6] a) X. Chen, L. Yu, S. Wang, D. Deng, X. Bao, *Nano Energy* **2017**, *32*, 353–358; b) P. Yin, T. Yao, Y. Wu, L. Zheng, Y. Lin, W. Liu, H. Ju, J. Zhu, X. Hong, Z. Deng, G. Zhou, S. Wei, Y. Li, *Angew. Chem. Int. Ed.* **2016**, *55*, 10800–10805; *Angew. Chem.* **2016**, *128*, 10958–10963; c) Y. Chen, S. Ji, Y. Wang, J. Dong, W. Chen, Z. Li, R. Shen, L. Zheng, Z. Zhuang, D. Wang, Y. Li, *Angew. Chem. Int. Ed.* **2017**, *56*, 6937–6941; *Angew. Chem.* **2017**, *129*, 7041–7045.

[7] a) H. Zhang, J. Wei, J. Dong, G. Liu, L. Shi, P. An, G. Zhao, J. Kong, X. Wang, X. Meng, J. Zhang, J. Ye, *Angew. Chem. Int. Ed.* **2016**, *55*, 14310–14314; *Angew. Chem.* **2016**, *128*, 14522–14526; b) S. Back, Y. Jung, *ACS Energy Lett.* **2017**, *2*, 969–975.

[8] S. Liang, B. Qiao, X. Song, C. Hao, A. Wang, T. Zhang, Y. Shi, *Nano Energy* **2017**, DOI: https://doi.org/10.1016/j.nanoen.2017.06.036.

[9] Y. Zheng, Y. Jiao, Y. Zhu, Q. Cai, A. Vasileff, L. H. Li, Y. Han, Y. Chen, S.-Z. Qiao, *J. Am. Chem. Soc.* **2017**, *139*, 3336–3339.

[10] a) G. Xu, H. Wei, Y. Ren, J. Yin, A. Wang, T. Zhang, *Green Chem.* **2016**, *18*, 1332–1338; b) G. Vilé, D. Albani, M. Nachtegaal, Z. Chen, D. Dontsova, M. Antonietti, N. López, J. Pérez-Ramírez, *Angew. Chem. Int. Ed.* **2015**, *54*, 11265–11269; *Angew. Chem.* **2015**, *127*, 11417–11422; c) L. Lin, W. Zhou, R. Gao, S. Yao, X. Zhang, W. Xu, S. Zheng, Z. Jiang, Q. Yu, Y.-W. Li, C. Shi, X.-D. Wen, D. Ma, *Nature* **2017**, *544*, 80–83.

[11] a) A. Wang, T. Zhang, *Nat. Energy* **2016**, *1*, 15019; b) C. Zhu, S. Fu, Q. Shi, D. Du, Y. Lin, *Angew. Chem. Int. Ed.* **2017**, DOI: https://doi.org/10.1002/anie.201703864; *Angew. Chem.* **2017**, DOI: https://doi.org/10.1002/ange.201703864; c) B. Bayatsarmadi, Y. Zheng, A. Vasileff, S.-Z. Qiao, *Small* **2017**, *13*, 1700191; d) Y. Li, S. Chen, R. Long, H. Ju, Z. Wang, X. Yu, F. Gao, Z. Cai, C. Wang, Q. Xu, J. Jiang, J. Zhu, L. Song, *Nano Energy* **2017**, *34*, 306–312.

[12] a) H. J. Qiu, Y. Ito, W. Cong, Y. Tan, P. Liu, A. Hirata, T. Fujita, Z. Tang, M. Chen, *Angew. Chem. Int. Ed.* **2015**, *54*, 14031–14035; *Angew. Chem.* **2015**, *127*, 14237–14241; b) N. Cheng, S. Stambula, D. Wang, M. N. Banis, J. Liu, A. Riese, B. Xiao, R. Li, T.-K. Sham, L.-M. Liu, G. A. Botton, X. Sun, *Nat. Commun.* **2016**, *7*, 13638; c) L. Fan, P. F. Liu, X. Yan, L. Gu, Z. Z. Yang, H. G. Yang, S. Qiu, X. Yao, *Nat. Commun.* **2016**, *7*, 10667.

[13] a) H. Fei, J. Dong, M. J. Arellano-Jiménez, G. Ye, N. Dong Kim, E. L. G. Samuel, Z. Peng, Zhu, Z. F. Qin, J. Bao, M. J. Yacaman, P. M. Ajayan, D. Chen, J. M. Tour, *Nat. Commun.* **2015**, *6*, 8668; b) J. Deng, H. Li, J. Xiao, Y. Tu, D. Deng, H. Yang, H. Tian, J. Li, P. Ren, X. Bao, *Energy Environ. Sci.* **2015**, *8*, 1594–1601; c) S. T.

Hunt, M. Milina, Z. Wang, Y. Roman-Leshkov, *Energy Environ. Sci.* **2016**, *9*, 3290 – 3301.
[14] a) K. Li, J. Zhang, R. Wu, Y. Yu, B. Zhang, *Adv. Sci.* **2016**, *3*, 1500426; b) B. Liu, L. Zhang, W. Xiong, M. Ma, *Angew. Chem. Int. Ed.* **2016**, *55*, 6725 – 6729; *Angew. Chem.* **2016**, *128*, 6837 – 6841.
[15] a) R. Chen, C. Yang, W. Cai, H.-Y. Wang, J. Miao, L. Zhang, S. Chen, B. Liu, *ACS Energy Lett.* **2017**, *2*, 1070 – 1075; b) S. Cherevko, A. A. Topalov, A. R. Zeradjanin, G. P. Keeley, K. J. J. Mayrhofer, *Electrocatalysis* **2014**, *5*, 235 – 240; c) J. Li, H.-M. Yin, X.-B. Li, E. Okunishi, Y.-L. Shen, J. He, Z.-K. Tang, W.-X. Wang, E. Yücelen, C. Li, Y. Gong, L. Gu, S. Miao, L.-M. Liu, J. Luo, Y. Ding, *Nat. Energy* **2017**, *2*, 17111.
[16] a) G. Dong, M. Fang, H. Wang, S. Yip, H.-Y. Cheung, F. Wang, C.-Y. Wong, S. T. Chu, J. C. Ho, *J. Mater. Chem. A* **2015**, *3*, 13080 – 13086; b) M. Tavakkoli, N. Holmberg, R. Kronberg, H. Jiang, J. Sainio, E. I. Kauppinen, T. Kallio, K. Laasonen, *ACS Catal.* **2017**, *7*, 3121 – 3130.
[17] a) Y. Kuang, G. Feng, P. Li, Y. Bi, Y. Li, X. Sun, *Angew. Chem. Int. Ed.* **2016**, *55*, 693 – 697; *Angew. Chem.* **2016**, *128*, 703 – 707; b) Y. P. Zhu, T. Y. Ma, M. Jaroniec, S.-Z. Qiao, *Angew. Chem. Int. Ed.* **2017**, *56*, 1324 – 1328; *Angew. Chem.* **2017**, *129*, 1344 – 1348; c) Y. P. Zhu, C. Guo, Y. Zheng, S.-Z. Qiao, *Acc. Chem. Res.* **2017**, *50*, 915 – 923; d) J. Duan, S. Chen, A. Vasileff, S.-Z. Qiao, *ACS Nano* **2016**, *10*, 8738 – 8745; e) Y. Zheng, Y. Jiao, Y. Zhu, L. H. Li, Y. Han, Y. Chen, M. Jaroniec, S.-Z. Qiao, *J. Am. Chem. Soc.* **2016**, *138*, 16174 – 16181.
[18] F. Dvořák, M. Farnesi Camellone, A. Tovt, N.-D. Tran, F. R. Negreiros, M. Vorokhta, T. Skála, I. Matolínová, J. Mysliveček, V. Matolín, S. Fabris, *Nat. Commun.* **2016**, *7*, 10801.
[19] X. Huang, Z. Zhao, L. Cao, Y. Chen, E. Zhu, Z. Lin, M. Li, A. Yan, A. Zettl, Y. M. Wang, X. Duan, T. Mueller, Y. Huang, *Science* **2015**, *348*, 1230 – 1234.
[20] a) I. Ledezma-Yanez, W. D. Z. Wallace, P. Sebastián-Pascual, V. Climent, J. M. Feliu, M. T. M. Koper, *Nat. Energy* **2017**, *2*, 17031; b) Y. Zheng, Y. Jiao, M. Jaroniec, S.-Z. Qiao, *Angew. Chem. Int. Ed.* **2015**, *54*, 52 – 65; *Angew. Chem.* **2015**, *127*, 52 – 66.
[21] Y. Jiao, Y. Zheng, K. Davey, S.-Z. Qiao, *Nat. Energy* **2016**, *1*, 16130.

Manuscript received: July 7, 2017
Accepted manuscript online: August 8, 2017
Version of record online: August 23, 2017

